HHS Public Access

Author manuscript

*J Invest Dermatol*. Author manuscript; available in PMC 2022 April 01.

Published in final edited form as:

*J Invest Dermatol*. 2021 April ; 141(4): 903–912.e4. doi:10.1016/j.jid.2020.08.023.

# The HDAC Inhibitor Domatinostat Promotes Cell Cycle Arrest, Induces Apoptosis and Increases Immunogenicity of Merkel Cell Carcinoma Cells

**Lina Song**[1,2], **Anne Catherine Bretz**[3], **Jan Gravemeyer**[1,2,4], **Ivelina Spassova**[1,2], **Shakhlo Muminova**[1,2,4], **Thilo Gambichler**[5], **Ashwin Sriram**[1,2,4], **Soldano Ferrone**[6], **Jürgen C. Becker**[1,2,4]

[1]Department of Translational Skin Cancer Research, Dermatology, University Hospital Essen

[2]German Cancer Consortium (DKTK), Partner Site Essen

[3]4SC AG, Planegg-Martinsried, Germany

[4]German Cancer Research Center (DKFZ), Heidelberg, Germany

[5]Ruhr-University Bochum, Bochum, Germany

[6]Division of Surgical Oncology, Department of Surgery, Massachusetts General Hospital, Harvard Medical School, Boston, MA, USA.

## Abstract

Merkel cell carcinoma (MCC) is a rare, highly aggressive skin cancer for which immune modulation by immune checkpoint inhibitors show remarkable response rates. However, primary or secondary resistance to immunotherapy prevents benefits in a significant proportion of patients. For MCC, one immune escape mechanism is insufficient recognition by T cells due to downregulation of major histocompatibility complex (MHC) class I surface expression. Histone deacetylase (HDAC) inhibitors have been demonstrated to epigenetically reverse low MHC class I expression caused by downregulation of the antigen processing machinery (APM). Domatinostat, an orally available small molecule inhibitor targeting HDAC class I, is currently in clinical evaluation to overcome resistance to immunotherapy. Here, we present preclinical data on its efficacy and mode of action in MCC. Single-cell RNA-sequencing revealed a distinct gene

To whom correspondence should be addressed: Jürgen C. Becker, Department of Translational Skin Cancer research, Universitätsstraße 1, S05 T05 B24, Essen 45141, Germany. Phone: +49 201-1836727, j.becker@dkfz.de, Fax: +49 201-1836945.

AUTHOR CONTRIBUTIONS

**Conception and design:** L. Song, J.C. Becker

**Development of methodology:** L. Song, J. Gravemeyer, S. Ferrone, J.C. Becker

**Analysis and interpretation of data (e.g., statistical analysis, biostatistics, computational analysis):** L. Song, A.C. Bretz, J. Gravemeyer, A. Sriram, J.C. Becker

**Writing, review, and/or revision of the manuscript:** L. Song, A.C. Bretz, J. Gravemeyer, A. Sriram, Ivelina Spassova, Shakhlo Muminova, Thilo Gambichler, S. Ferrone, J.C. Becker

**Study supervision:** J.C. Becker

CONFLICT OF INTEREST

None of other authors indicated any potential conflicts of interest.

expression signature of antigen processing and presentation, cell cycle arrest and execution phase of apoptosis upon treatment. Accordingly, functional assays showed that it induced G2M arrest and apoptosis. In surviving cells, APM component gene transcription and translation were up-regulated, consequently resulting in increased MHC class I surface expression. Altogether, domatinostat not only exerts direct anti-tumoral effects, but also restores HLA class I surface expression on MCC cells. Therefore, restoring surviving MCC cells' susceptibility to recognition and elimination by cognate cytotoxic T cells.

**Keywords**

Merkel cell carcinoma; histone deacetylase inhibitor; antigen presentation; cell cycle arrest; apoptosis; cell viability

## INTRODUCTION

Merkel cell carcinoma (MCC) is an aggressive neuroendocrine skin cancer, occurring preferentially in elderly or immune-compromised patients. MCC is either associated with genomic integration of the Merkel cell polyomavirus (MCPyV) or chronic UV exposure (Becker et al., 2017). It typically manifests as a rapidly developing, painless tumor on sun-exposed areas of the skin.

Until recently, the prognosis for patients with advanced MCC not amendable by surgery or radiation was gloomy. This dramatically changed with the introduction of immunotherapy by immune checkpoint inhibitors, *i.e.*, antibodies blocking programmed cell death protein 1 (PD-1) or programmed cell death protein ligand 1 (PD-L1), which demonstrate remarkable clinical activity (Kaufman et al., 2018; Nghiem et al., 2019). Unfortunately, about half of the patients either show primary or develop secondary resistance to immune checkpoint inhibitors (Spassova et al., 2020). Recent studies demonstrated that one immune evasion mechanism is represented by reduced or lack of major histocompatibility complex (MHC) class I surface expression (Paulson et al., 2014; Paulson et al., 2018; Ritter et al., 2017). Loss of MHC class I surface expression may be due to impaired HLA gene expression (Raffaghello et al., 2005), lack of $\beta_2$-microglobulin (β2m) expression (Sade-Feldman et al., 2017) or MHC class I molecule instability because of lack of peptide binding to HLA class I groove (Ritter et al., 2017). The latter is caused by defective expression and/or function of the antigen processing and presentation machinery (APM) (Cai et al., 2018).

Histone deacetylases (HDACs) are a specific class of enzymes that catalyze the deacetylation of proteins, in particular histones. HDACs are categorized in four classes depending on sequence homology to the yeast enzymes and their domain organization. Class I HDACs are primarily present in the nucleus, whereas the other classes are found both in the nucleus and the cytoplasm (Kong et al., 2011). Aberrant expression and regulation of HDACs is often found in cancer, suggesting a critical role of these enzymes in tumorigenesis (Li and Seto, 2016). Similarly, disparate acetylation of non-histone proteins involved in cell cycle and apoptosis regulation is normalized upon HDAC inhibition (Li et al., 2016). Furthermore, several lines of evidence suggest an immunogenic impact of HDAC inhibition (Conte et al., 2018) such as induction of cancer germline antigens (Moreno-Bost et al.,

2011), T cell recruiting chemokines (Zheng et al., 2016) and APM component genes (Setiadi et al., 2008). Indeed, we have previously reported that in both MCC cell lines and in tumor tissues, reduced APM component gene expression can be normalized by broad-spectrum HDAC inhibitors such as vorinostat or panobinostat (Ritter et al., 2017; Ugurel et al., 2019).

The clinical use of broad spectrum HDAC inhibitors is well established (West et al., 2014). However, HDAC class I inhibitors are currently regarded as even more promising agents for the treatment of cancer, mainly due to a strong induction of cell cycle arrest (Ververis et al., 2013). Hence, we scrutinized the effects of domatinostat (aka 4SC-202), an orally available small molecule inhibitor selectively targeting class I HDACs (HDAC 1, 2 and 3), since it is currently be tested in the treatment of advanced MCC patients in combination with the anti-PD-L1 antibody avelumab (NCT04393753)[1]. Domatinostat also inhibits the lysine-specific histone demethylase 1A (LSD1) and the repressor element 1 (RE1)-silencing transcription factor/neuron-restrictive silencer factor (REST/NRSF) at low μM concentrations (von Tresckow et al., 2019; Inui et al., 2017). Notably, dysregulation REST expression had been associated with the neuroendocrine differentiation of MCC cells (Chteinberg et al., 2018). Albeit this may explain some of the differences of domatinostat's activity as compared to other HDAC inhibitors, its true work mechanism is yet not fully established (Haydn et al., 2017). To add some additional information on domatinostat's impact on neoplastic cells, we report here that it causes G2M arrest and apoptosis in a fraction of MCC cells; in the remaining viable cells, it strongly induces APM component gene transcription resulting in increased HLA class I surface expression.

## RESULTS

### Domatinostat induces a distinct gene expression pattern in MCC cells

The effect of domatinostat treatment on the transcriptome was scrutinized in the classical MCC cell line WaGa. Cells were treated with domatinostat at a concentration of 2.5 μM for 24 hours at 37°C. In line with earlier evidence of epigenetic landscaping and transcriptional regulation by HDAC inhibitors (Halsall et al., 2015; Hull et al., 2016; Ritter et al., 2017), single-cell RNA-sequencing (scRNA-seq) and subsequent cluster assignment revealed a distinct gene signature upon domatinostat treatment (Figure 1a). scRNA-seq revealed significant differential expression of 63 genes (adjusted p-value < 0.1) (Figure 1b). Functional annotation and pathway enrichment analysis of these differentially expressed genes defined 12 biological processes and/or molecular functions including antigen processing and presentation, apoptosis, transport along microtubule, epithelial cell migration and circadian rhythm (Figure 1c). In the following studies, we particularly focused on cell cycle and apoptosis regulation, as well as APM.

### Induction of G2M cell cycle arrest

Previous reports suggested that HDAC inhibition induces G2M cell cycle arrest in cancer cells (Dong et al., 2018). Annotating our scRNA-seq data according to cell cycle phases

[1]Bartz R, Behling T, Reimann P, Hermann F. Preclinical rationale and clinical design for the combination of domatinostat with avelumab in Merkel Cell Carcinoma patients: the MERKLIN and MERKLIN 2 studies. 1st International Symposium on Merkel Cell Carcinoma; 21. – 22. Oct. 2019, Tampa, Florida, USA

revealed a more than 1.4-fold increase in number of cells with a gene expression signature for G2M cell cycle phase upon domatinostat treatment (Figure 2a). Gene Set Enrichment Analysis (GSEA) demonstrated hallmark of G2M checkpoint gene signature (Figure 2b). To functionally test this observation, we performed BrdU incorporation assays at three time points (24 hours, 48 hours and 72 hours) for three MCPyV-positive MCC cell lines (WaGa, MKL-1, MKL-2) and one MCPyV-negative MCC cell line (UM-MCC34). Cells were synchronized to G1 phase using serum starvation prior to these experiments (Figure S1). The cell cycle determination revealed that G2M cell cycle arrest was observed already after 24 hours of domatinostat treatment but being most pronounced after 48 hours. The well-known cell cycle inhibitor nocodazole, used as a positive control, also resulted in a G2M arrest after treatment (Figure 2c, Figure S2). Quantification of cells in the respective cell cycle phases determined in a series of experiments (n=3), demonstrated a 4-fold increase in the number of cells in G2M phase after domatinostat and a 6-fold increase after nocodazole treatment for 48 hours (Figure 2d). For fibroblasts, we did not observe G2M arrest.

## Induction of apoptosis

HDAC inhibitors are potent inducers of apoptosis in cancer cells (Bolden et al., 2006; Lei et al., 2010). Persistent G2M arrest of cells may cause their apoptosis (Tyagi et al., 2002; Wang et al., 2016). Furthermore, domatinostat modulated the expression of apoptotic genes in WaGa cells (Figure 1c). Thus, we next evaluated the impact of domatinostat on cell viability. Indeed, domatinostat treatment reduced the fraction of viable MCC cells, whereas primary fibroblasts were not affected (Figure 3a). Specifically, domatinostat induced apoptosis in WaGa, MKL-1, MKL-2 and UM-MCC34 cells as detected by an increase in caspase 3/7 activity and the loss of mitochondrial membrane potential ($\Delta\Psi_m$). Notably, MCC cell lines growing as spheroids dissociated upon treatment (Figure 3d). Forty-six percent of WaGa, 65.4 % of MKL-1, 22.13 % of MKL-2 and 21.1% of UM-MCC34 cells underwent apoptosis upon treatment with domatinostat within 24 hours. Again, nocodazole served as positive control; despite the fact that it was more effective to induce G2M arrest, it induced less apoptosis (Figure 3b-d, Figure S3a). It should be noted that the fibroblasts, which died neither after treatment with domatinostat nor nocodazole (Figure 3a-d, Figure S3a), were susceptible to $H_2O_2$ induced apoptosis as previously described (Xiang et al., 2016) (Figure S3b–d).

## Increased expression of APM genes and MHC class I surface molecules

scRNA-seq analysis demonstrated a domatinostat-induced expression of APM genes in living WaGa cells. We wanted to confirm this observation in additional MCC cell lines. Since domatinostat induced apoptosis in a substantial fraction of, but not all MCC cells, we quantified APM component gene expression in surviving cells, *i.e.*, after enrichment of viable cells. We scrutinized the expression of transporter associated with antigen processing 1 and 2 (TAP1 and TAP2), as well as large multifunctional protease 2 and 7 (LMP2 and LMP7). The induction of these genes and proteins upon treatment with another HDAC inhibitor in MCC was previously reported (Ritter et al., 2017). First, the kinetics of induction of these APM component genes were tested by time course experiments measuring LMP2 and TAP2 mRNA expression in WaGa cells. Four, 8 and 24 hours after treatment with variable domatinostat concentrations were performed. These experiments demonstrated the

induction of mRNA expression of these genes after 24 hours in a dose-dependent manner (Figure 4a).

The condition demonstrating significant efficacy was used for additional experiments (2.5 μM/24 hours). All of the APM component genes analyzed (LMP2, LMP7, TAP1 and TAP2) were significantly upregulated in the viable cell fraction following treatment with domatinostat (Figure 4b). As domatinostat specifically augments APM component gene expression in viable cells, the upregulation of APM component genes is unlikely to be just a consequence of decreased cell viability, as has been described for some forms of immunogenic cell death (Zhou et al., 2019). Immunoblots for TAP1, TAP2, LMP2 and LMP7 proteins confirmed the increased expression of all of them upon domatinostat treatment. Furthermore, this induction was paralleled by an increased expression of β2-microglobulin and HLA-A (Figure 4c).

To test whether HLA class I proteins are expressed in a functional manner and subsequently transported to the plasma membrane, mAb W6/32 targeting HLA class I (Ravindranath et al., 2017) was used to detect cell surface expression by flow cytometry in non-permeabilized MCC cells and primary fibroblasts. In accordance to the results obtained with whole cell lysates (Figure 4c), basal expression of HLA class I was low in three MCC cell lines WaGa, MKL-1 and UM-MCC34. Thus, domatinostat induced an increase of HLA class I surface expression specifically in MCC cells in a concentration-dependent manner (Figure 4d, e).

## DISCUSSION

Notwithstanding the excellent clinical activity of immune therapy with immune checkpoint inhibitors in MCC, a substantial number of patients do not benefit due to primary or secondary resistance (Kaufman et al., 2018; Nghiem et al., 2019). We have previously shown that this may be caused by impaired HLA class I cell surface expression, which impedes recognition of MCC cells by cognate cytotoxic T-cells (Paulson et al., 2014; Ritter et al., 2017). The impaired HLA class I cell surface expression can be restored by the broad-spectrum HDAC inhibitor vorinostat in combination with the Sp1-inhibitor mithramycin A (Ritter et al., 2017). Moreover, broad-spectrum HDAC inhibition by panobinostat enhanced HLA class I surface expression on tumor cells resulting in a brisk infiltration by $CD8^+$ T cells in a patient refractory to immune checkpoint inhibitor therapy (Ugurel et al., 2019).

Based on these observations, it appears attractive to combine HDAC inhibitors with immunotherapy (Harms et al., 2018). Indeed, currently the class I HDAC inhibitor domatinostat in combination with the anti-PD-L1 antibody avelumab is tested as first and second line therapy of advanced MCC (MERKLIN 1 and 2; NCT04393753). To provide the requirements for a rational design of translational studies for the MERKLIN trials, we specifically scrutinized the effects of domatinostat on MCC cells *in vitro*.

Domatinostat is highly specific for HDAC 1–3 with inhibitory constant (Ki) values in the nM range. It is also an inhibitor for the histone demethylase LSD1, which is demonstrated to be a regulator of a wide spectrum of biological processes, involved in cancer development and progression (von Tresckow et al., 2019). Concomitant targeting of HDAC and LSD1

proved to be a promising strategy for the cancer treatment as it induces apoptosis by shifting the balance of anti- and pro-apoptotic BCL-2 family proteins (Haydn et al., 2017). However, the dual inhibitory activity of domatinostat has not been scrutinized yet and requires additional experiments (von Tresckow et al., 2019).

Domatinostat causes a G2M cell cycle arrest and initiates apoptosis in MCC cells. Interestingly, domatinostat induced G2M phase arrest in synchronized MCC cells already after 24 hours and most pronounced at 48 hours. This observation is remarkable since MCC cell lines have a rather long doubling time (Schrama et al., 2019). However, doubling time in cell culture not only reflects the duration of the cell cycle, but also the amount of cell death. Indeed, in MCC tissues, both a high mitotic as well as a high apoptotic rate is observed (Becker et al., 2017). To functionally address this notion, nocodazole, which induces both G2M arrest and apoptosis, was used as comparator in the cell cycle and apoptosis experiments in cells synchronized to G1 phase. Similar to domatinostat, MCC cells were arrested in G2M phase already after 24 hours of treatment. However, less apoptosis was observed in nocodazole treated MCC cells; thus, domatinostat may also specifically kill MCC cells by directly inducing apoptosis. Furthermore, scRNA-seq identified transcriptional modulation patterns caused by domatinostat in MCC, among which the apoptosis signature was most prominent. The observed effects of domatinostat were specific to MCC cells, whereas fibroblasts were unaffected. This is in line with the hypothesis that cancer cells, in contrast to normal cells, are more susceptible to HDAC inhibition as they require low acetylation levels and thus strongly depend on HDAC activity for maintenance of oncogenic phenotype (Cavalli and Heard, 2019).

HDACs are a set of enzymes that can be used to catalyze the deacetylation of proteins, resulting in changes in protein stability or gene expression. HDACs are classified into three categories: class I (HDACs 1–3 and 8), class II (IIa: HDACs 4, 5, 7 and 9; IIb: HDACs 6 and 10) and class IV (HDAC 11) (Haberland et al., 2009). Based on the predominance of class I enzymes in cancer cells (Glaser et al., 2003), it is assumed that class I-specific HDAC inhibitors may supersede clinical effects of broad-spectrum inhibitors (Karagiannis and El-Osta, 2006). Indeed, the anti-tumoral activity of class I HDAC inhibitors in hematological malignancies and pediatric tumors have been described (von Tresckow et al., 2019). In medulloblastoma, domatinostat treatment inhibits cell viability and downregulates hedgehog signaling significantly. Upregulated proteins such as HDAC2 and HDAC3 are key targets for domatinostat in medulloblastoma (Messerli et al., 2017).

Importantly, induction of cell cycle arrest and apoptosis of tumor cells is not the only modus operandi of domatinostat. In viable cells, we observed a strong induction of components of the APM resulting in an increased MHC class I surface expression. Thus, domatinostat is counteracting one of the major immune escape mechanisms of MCC (Ritter et al., 2017). This observation explains previous reports, that Domatinostat enhances the infiltration of cytotoxic T cells into tumors of syngeneic mouse models resulting in synergistic effects when combined with immune checkpoint blocking antibodies (Hamm et al., 2018). Moreover, Bretz et al. (2019), recently investigated the changes in immune gene expression signatures by RNA-seq of patient samples obtained in the SENSITIZE trial (NCT03278665). This trial evaluates the efficacy of domatinostat combined with

pembrolizumab in advanced-stage melanoma patients refractory/non-responding to prior PD-1 blockade. The results from these analyses revealed an increased expression of APM and MHC genes, along with an upregulation of IFN-γ signaling and recently described pembrolizumab response gene signature (Ayers et al., 2017). In summary, we provide several lines of evidence suggesting that the class I-selective HDAC inhibitor domatinostat may be effective in MCC patients. On one hand, domatinostat induces cell cycle arrest and apoptosis, on the other hand, it boosts antigen presentation in viable cells. In line with this, it has been recently reported that domatinostat increased expression of cancer germline antigens and MHC molecules on cancer cells *in vitro* and *in vivo*. Thus, in syngeneic colorectal models, it induces infiltration of cytotoxic T cells into the tumor microenvironment and synergizes with immune checkpoint inhibitors treatment (Bretz et al., 2019). However, the relevance of the different working mechanisms of domatinostat and other HDACi are not fully understood. Still, our observations add to the rationale of a combined therapeutic approach of domatinostat along with checkpoint inhibitors for MCC therapy. Accordingly, clinical trials are already in its initiation phase.

## MATERIAL AND METHODS

### cell lines and cell culture

MCC cell lines WaGa, MKL-1, MKL-2 and UM-MCC34 have been described before (Houben et al., 2010; Fan et al., 2018) All cell lines were cultured under standard conditions (37 °C; 5% CO2) in RPMI-1640 medium (PAN Biotech, Aidenbach, Germany) supplemented with 10% fetal bovine serum (FBS; PAN Biotech), 1% penicillin-streptomycin (P/S; PAN Biotech). Primary skin fibroblasts isolated from healthy skin were cultured in DMEM and DMEM/F12 (1:1) medium (Lonza, Cologne, Germany) supplemented with 10% FBS and 1% P/S. Cell lines were regularly tested to ensure absence of mycoplasma and their identity was regularly verified by DNA fingerprinting (last performed in June 2019).

For treatment with domatinostat (4SC AG, Planegg-Martinsried, Germany) or nocodazole (Sigma-Aldrich, Darmstadt, Germany), cells were seeded in 6-well plates at a concentration of $1\times10^6$ cells/ml. Domatinostat was dissolved in DMSO (PanReac AppliChem, Darmstadt, Germany). Domatinostat and nocodazole were used at the indicated concentrations. To quantify the number of viable cells, trypan blue exclusion assay was used. Dead cells were removed by Ficoll-Paque (Biochrom, Berlin, Germany) density centrifugation.

### scRNA-seq and gene expression analysis

MCC cells were single-cell barcoded using the 10x Genomics 3’ Chromium v2.0 platform (Zheng et al., 2017). Library preparation was performed according to the 10x Genomics protocol. The libraries were sequenced on an Illumina HiSeq 4000. The Cell Ranger Single Cell Software Suite version 2.1.1 (http://10xgenomics.com/) was used with default settings to separately align cDNA reads to the hg19 human reference genome. Data were then aggregated into one file and imported into the Loupe browser v2.0.0 (http://10xgenomics.com/) and R. Single-cell gene expression was visualized by UMAP for dimension reduction.

For cell cycle annotation, signatures were calculated using marker genes reported by Kowalczyk et al (Kowalczyk et al., 2015). Pathway analysis of significantly regulated genes (adjusted P-value < 0.1) was performed with Metascape (http://metascape.org) using default settings. For gene set enrichment analysis (GSEA), GSEA version 3.0 was used (Subramanian et al, 2005). Pre-ranked analyses were performed by sorting differentially expressed genes according to their logarithm fold changes (lnFC) without prior filtering on significance or effect size. Enrichment was then tested for the hallmark of cancer gene set (Subramanian et al., 2005).

### Cell cycle synchronization and cell cycle analysis

For cell cycle synchronization, MCC cell lines and primary fibroblasts were seeded in 6-well plates and cultured for 24, 48 and 72 hours without serum before the incorporation rate of Bromodesoxyuridine (BrdU) was measured. Cells were pulse-labeled with BrdU (2.5 μg/mL, BioLegend, Koblenz, Germany) 2 hours before harvest. Subsequently, cells were washed with PBS and fixed with 70 % ethanol for 30 minutes on ice. After denaturation with 1.5 M HCl for 30 minutes at room temperature (RT), cells were washed with PBS (PAN Biotech) and stained with a FITC-labeled anti-BrdU monoclonal antibody (clone 3D4, Biolegend) for 30 minutes at RT. Prior to flow cytometric analysis, 1 μL of 7-aminoactinomycin (7-AAD; 10 μg/ml, Abcam, Berlin, Germany) was added. Ten thousand events were analyzed on a flow cytometer (Cytoflex, Beckman Coulter Life Science, Krefeld, Germany) and gates were adjusted to quantify cell cycle populations (G0/G1, S, G2M). Data were analyzed using FlowJo TM V10.6.1 (Becton Dickinson (BD), Franklin Lakes, USA).

### Cell viability assays

CellTiter 96® Aqueous One Solution Cell Viability Assay (Promega, Mannheim, Germany) was used to measure the viability of MCC cells and primary fibroblasts. The cells were grown in 96-well plates 24 hours prior to treatment. Cells were treated with indicated concentrations. After 24 hours, 20 μL of CellTiter 96® $AQ_{ueous}$ One Solution Cell Proliferation Assay reagent were added to each well and cells were then incubated for 120 min at 37 °C before absorbance was measured at 490 nm using a Spectramax microplate reader (Molecular Devices, LLC, San Jose, CA, USA).

### Apoptosis assays

To determine cellular apoptosis, the NucView 488/MitoView 633 Apoptosis Assay Kit (Biotium, Fremont, United States) was used according to the manufacturer's instructions. Viable and apoptotic cells were visualized by fluorescence microscopy (Zeiss Axio Observer.Z1, Oberkochen, Germany) and quantified by flow cytometry. Data were analyzed using the CytExpert version 2.3 software (Beckman Coulter, Krefeld, Germany).

### Quantitative real time polymerase chain reaction (qRT-PCR)

RNA was isolated using PeqGOLD total RNA kit (VWR/Peqlab, Erlangen, Germany) and transcribed into cDNA using the SuperScript IV reverse transcriptase (ThermoFisher, Dreieich, Germany) according to the manufacturer's instructions. qRT-PCR was performed

on the CFX Real-Time PCR system (Bio-Rad Laboratories, Düsseldorf, Germany). RPLP0 served as an endogenous control and was detected with specific primers and a TaqMan probe: 6-FAM-YY-ATCTGCTGCATCTGCTTGGAGCCCA-BHQ1 (Applied Biosystems, Darmstadt, Germany). The mRNA expression of TAP1, TAP2, LMP2 (PSMB9) and LMP7 (PSMB8) was detected using SYBR green assays (Sigma-Aldrich, Darmstadt, Germany) with primers listed in Supplementary Table 1. Relative quantification was calculated by the ΔΔCt method.

### Immunoblotting

Cell lysates were generated as described before (Skov et al., 2005). 4–12% Bis-Tris plus precast gels (ThermoFisher) were used for protein electrophoresis. Samples were then transferred to nitrocellulose membranes using iBlot dry blotting system (ThermoFisher). The nitrocellulose membranes were blocked for 1 hour with 5% BSA in TBST (TBS with 0.05% Tween 20) and incubated overnight at 4 °C with the respective primary antibodies: Anti-HLA heavy chain (clone EP1395Y, Abcam, 1:4000), anti-β-tubulin (clone TUB2.1, Sigma Aldrich, 1:200), anti- β2m (1:500), anti-TAP1 (1:500), anti-TAP2 (1:500), anti-LMP2 (1:500) and anti-LMP7 (1:500). TAP1, TAP2, LMP2 and LMP7 specific mAbs have been produced and characterized as described elsewhere (Wang et al., 2005). The following day, membranes were washed and incubated for 1 hour with the appropriate peroxidase-coupled secondary antibodies (Agilent Technologies, Ratingen, Germany), followed by visualization using the Plus-ECL chemiluminescence detection kit (ThermoFisher).

### Flow cytometry

Cell surface expression of HLA class I proteins was determined by flow cytometry as described elsewhere (Ritter et al., 2017). Briefly, $1\times10^6$ cells were incubated with a FITC-conjugated anti-HLA class I antibody (clone W6/32, BioLegend) in PBS supplemented with 0.1% bovine serum albumin (BSA) for 90 minutes at 4°C in the dark. After three washes, cells were stained with 1 μL of 7-AAD for viable/non-viable cell discrimination and analyzed on flow cytometer. Cells were gated for singlets (FSC-A vs. FSC-H) and living cells (PC5.5A vs. FSC-A). Data were analyzed using FlowJo V10.

### Data Availability Statement

Datasets of single cell RNA sequencing of the MCC cell line WaGa upon domatinostat treatment compared to untreated WaGa control cells were uploaded to NCBI-GEO (GSE141832).

## Supplementary Material

Refer to Web version on PubMed Central for supplementary material.

## ACKNOWLEDGEMENTS

This work was funded by Deutsches Konsortium für Translationale Krebsforschung (DKTK) by ED003 and L. Song was supported by China Scholarship Council (CSC). S. Ferrone was supported in part by NIH grants CA 219603 and DE028172. The authors like to express their appreciation for the help from University Hospital Essen.

J.C. Becker is receiving speaker's bureau honoraria from Amgen, Pfizer, MerckSerono, Recordati and Sanofi, is a paid consultant/advisory board member for eTheRNA, MerckSerono, Pfizer, 4SC, Recordati, InProTher and Sanofi. His group receives research grants from Bristol-Myers Squibb, Merck Serono, and Alcedis. Anne Catherine Bretz is an employee of 4SC. S. Ferrone receives a research grant from Merck.

## ABBREVIATIONS:

| | |
|---|---|
| **APM** | antigen processing and presentation machinery |
| **HDAC** | histone deacetylase |
| **HLA** | human leukocyte antigen |
| **LMP** | large multifunctional protease |
| **MCC** | Merkel cell carcinoma |
| **MCPyV** | Merkel cell polyomavirus |
| **MHC** | major histocompatibility complex; scRNA-seq, single-cell RNA sequencing |
| **TAP** | transporter associated with antigen processing |

## REFERENCES

Ayers M, Lunceford J, Nebozhyn M, Murphy E, Loboda A, Kaufman DR, et al. IFN-gamma-related mRNA profile predicts clinical response to PD-1 blockade. J Clin Invest 2017;127(8):2930–40. [PubMed: 28650338]

Becker JC, Stang A, DeCaprio JA, Cerroni L, Lebbe C, Veness M, et al. Merkel cell carcinoma. Nat Rev Dis Primers 2017;3:17077.

Bolden JE, Peart MJ, Johnstone RW. Anticancer activities of histone deacetylase inhibitors. Nat Rev Drug Discov 2006;5(9):769–84. [PubMed: 16955068]

Bretz AC, Parnitzke U, Kronthaler K, Dreker T, Bartz R, Hermann F, et al. Domatinostat favors the immunotherapy response by modulating the tumor immune microenvironment (TIME). J Immunother Cancer 2019;7(1):294. [PubMed: 31703604]

Cai L, Michelakos T, Yamada T, Fan S, Wang X, Schwab JH, et al. Defective HLA class I antigen processing machinery in cancer. Cancer Immunol Immunother 2018;67(6):999–1009. [PubMed: 29487978]

Cavalli G, Heard E. Advances in epigenetics link genetics to the environment and disease. Nature 2019;571(7766):489–99. [PubMed: 31341302]

Conte M, De Palma R, Altucci L. HDAC inhibitors as epigenetic regulators for cancer immunotherapy. Int J Biochem Cell Biol 2018;98:65–74. [PubMed: 29535070]

Chteinberg E, Sauer CM, Rennspiess D, Beumers L, Schiffelers L, Eben J, et al. Neuroendocrine key regulator gene expression in merkel cell carcinoma. Neoplasia 2018;20:1227–1235. [PubMed: 30414538]

Dong Z, Yang Y, Liu S, Lu J, Huang B, Zhang Y. HDAC inhibitor PAC-320 induces G2/M cell cycle arrest and apoptosis in human prostate cancer. Oncotarget 2018;9(1):512–23. [PubMed: 29416632]

Fan K, Ritter C, Nghiem P, Blom A, Verhaegen ME, Dlogosz A, et al. Circulating cell-free miR-375 as surrogate marker of tumor burden in Merkel cell carcinoma. Clin Cancer Res 2018; 24(23):5873–5882. [PubMed: 30061360]

Glaser KB, Li J, Staver MJ, Wei RQ, Albert DH, Davidsen SK. Role of class I and class II histone deacetylases in carcinoma cells using siRNA. Biochem Biophys Res Commun 2003;310(2):529–36. [PubMed: 14521942]

Haberland M, Montgomery RL, Olson EN. The many roles of histone deacetylases in development and physiology: implications for disease and therapy. Nat Rev Genet 2009;10(1):32–42. [PubMed: 19065135]

Halsall JA, Turan N, Wiersma M, Turner BM. Cells adapt to the epigenomic disruption caused by histone deacetylase inhibitors through a coordinated, chromatin-mediated transcriptional response. Epigenetics Chromatin 2015;8(1):29. [PubMed: 26380582]

Hamm S, Wulff T, Kronthaler K, Schrepfer S, Parnitzke U, Bretz AC, et al. 4SC-202 increases immunogenicity of tumor cells, induces infiltration of tumor microenvironment with cytotoxic T cells, and primes tumors for combinations with different cancer immunotherapy approaches. Cancer Res 2018;78(13).

Harms PW, Harms KL, Moore PS, DeCaprio JA, Nghiem P, Wong MKK, et al. The biology and treatment of Merkel cell carcinoma: current understanding and research priorities. Nat Rev Clin Oncol 2018;15(12):763–76. [PubMed: 30287935]

Haydn T, Metzger E, Schuele R, Fulda S. Concomitant epigenetic targeting of LSD1 and HDAC synergistically induces mitochondrial apoptosis in rhabdomyosarcoma cells. Cell Death Dis 2017;8(6):e2879-e.

Houben R, Shuda M, Weinkam R, Schrama D, Feng H, Chang Y, et al. Merkel cell polyomavirus-infected Merkel cell carcinoma cells require expression of viral T antigens. J Virol 2010;84(14):7064–72. [PubMed: 20444890]

Hull EE, Montgomery MR, Leyva KJ. HDAC Inhibitors as Epigenetic Regulators of the Immune System: Impacts on Cancer Therapy and Inflammatory Diseases. BioMed Res Int 2016;2016:8797206.

Inui K, Zhao Z, Yuan J, Jayaprakash S, Le LTM, Drakulic S, et al. Stepwise assembly of functional C-terminal REST/NRSF transcriptional repressor complexes as a drug target. Protein Sci 2017;26(5):997–1011. [PubMed: 28218430]

Karagiannis TC, El-Osta A. Will broad-spectrum histone deacetylase inhibitors be superseded by more specific compounds? Leukemia 2006;21:61. [PubMed: 17109024]

Kaufman HL, Russell JS, Hamid O, Bhatia S, Terheyden P, D'Angelo SP, et al. Updated efficacy of avelumab in patients with previously treated metastatic Merkel cell carcinoma after >/=1 year of follow-up: JAVELIN Merkel 200, a phase 2 clinical trial. J Immunother Cancer 2018;6(1):7. [PubMed: 29347993]

Kong Y, Jung M, Wang K, Grindrod S, Velena A, Lee SA, et al. Histone deacetylase cytoplasmic trapping by a novel fluorescent HDAC inhibitor. Mol Cancer Ther 2011;10(9):1591–9. [PubMed: 21697394]

Kowalczyk E, Filipiak-Strzecka D, Hamala P, Smiech N, Kasprzak JD, Kusmierek J, et al. Prognostic implications of discordant results of myocardial perfusion single-photon emission computed tomography and exercise ECG test in patients with stable angina. Adv Clin Exp Med 2015;24(6):965–71. [PubMed: 26771967]

Lei WW, Zhang KH, Pan XC, Wang DM, Hu Y, Yang YN, et al. Histone deacetylase 1 and 2 differentially regulate apoptosis by opposing effects on extracellular signal-regulated kinase 1/2. Cell Death Dis 2010;1(5):e44.

Li QQ, Hao JJ, Zhang Z, Hsu I, Liu Y, Tao Z, et al. Histone deacetylase inhibitor-induced cell death in bladder cancer is associated with chromatin modification and modifying protein expression: A proteomic approach. Int J Oncol 2016;48(6):2591–607. [PubMed: 27082124]

Li Y, Seto E. HDACs and HDAC inhibitors in cancer development and therapy. Cold Spring Harb Perspect Med 2016;6(10):a026831.

Messerli SM, Hoffman MM, Gnimpieba EZ, Kohlhof H, Bhardwaj RD. 4SC-202 as a potential treatment for the pediatric brain tumor Medulloblastoma. Brain Sci 2017;7(11).

Moreno-Bost A, Szmania S, Stone K, Garg T, Hoerring A, Szymonifka J, et al. Epigenetic modulation of MAGE-A3 antigen expression in multiple myeloma following treatment with the demethylation agent 5-azacitidine and the histone deacetlyase inhibitor MGCD0103. Cytotherapy 2011;13(5):618–28. [PubMed: 21171821]

Nghiem P, Bhatia S, Lipson EJ, Sharfman WH, Kudchadkar RR, Brohl AS, et al. Durable tumor regression and overall survival in patients with advanced Merkel Cell Carcinoma receiving pembrolizumab as first-line therapy. J Clin Oncol 2019;37(9):693–702. [PubMed: 30726175]

Paulson KG, Tegeder A, Willmes C, Iyer JG, Afanasiev OK, Schrama D, et al. Downregulation of MHC-I expression is prevalent but reversible in Merkel cell carcinoma. Cancer Immunol Res 2014;2(11):1071–9. [PubMed: 25116754]

Paulson KG, Voillet V, McAfee MS, Hunter DS, Wagener FD, Perdicchio M, et al. Acquired cancer resistance to combination immunotherapy from transcriptional loss of class I HLA. Nat Commun 2018;9(1):3868. [PubMed: 30250229]

Raffaghello L, Prigione I, Bocca P, Morandi F, Camoriano M, Gambini C, et al. Multiple defects of the antigen-processing machinery components in human neuroblastoma: immunotherapeutic implications. Oncogene 2005;24(29):4634–44. [PubMed: 15897905]

Ravindranath MH, Jucaud V, Ferrone S. Monitoring native HLA-I trimer specific antibodies in Luminex multiplex single antigen bead assay: Evaluation of beadsets from different manufacturers. J Immunol Methods 2017;450:73–80. [PubMed: 28782523]

Ritter C, Fan K, Paschen A, Reker Hardrup S, Ferrone S, Nghiem P, et al. Epigenetic priming restores the HLA class-I antigen processing machinery expression in Merkel cell carcinoma. Sci Rep 2017;7(1):2290. [PubMed: 28536458]

Sade-Feldman M, Jiao YJ, Chen JH, Rooney MS, Barzily-Rokni M, Eliane JP, et al. Resistance to checkpoint blockade therapy through inactivation of antigen presentation. Nat Commun 2017;8(1):1136. [PubMed: 29070816]

Schrama D, Sarosi EM, Adam C, Ritter C, Kaemmerer U, Klopocki E, et al. Characterization of six Merkel cell polyomavirus-positive Merkel cell carcinoma cell lines: Integration pattern suggest that large T antigen truncating events occur before or during integration. Int J Cancer 2019;145(4):1020–32. [PubMed: 30873613]

Setiadi AF, Omilusik K, David MD, Seipp RP, Hartikainen J, Gopaul R, et al. Epigenetic enhancement of antigen processing and presentation promotes immune recognition of tumors. Cancer Res 2008;68(23):9601–7. [PubMed: 19047136]

Skov S, Pedersen MT, Andresen L, Straten PT, Woetmann A, Odum N. Cancer cells become susceptible to natural killer cell killing after exposure to histone deacetylase inhibitors due to glycogen synthase kinase-3-dependent expression of MHC class I-related chain A and B. Cancer Res 2005;65(23):11136–45.

Spassova I, Ugurel S, Terheyden P, Sucker A, Hassel JC, Ritter C, et al. Predominance of central memory T cells with high T-cell receptor repertoire diversity is associated with response to PD-1/PD-L1 inhibition in Merkel cell carcinoma. Clin Cancer Res 2020; 2244.019.

Subramanian A, Tamayo P, Mootha VK, Mukherjee S, Ebert BL, Gillette MA, et al. Gene set enrichment analysis: A knowledge-based approach for interpreting genome-wide expression profiles. Proc Natl Acad of USA 2005;102(43):15545–50.

Tyagi AK, Singh RP, Agarwal C, Chan DC, Agarwal R. Silibinin strongly synergizes human prostate carcinoma DU145 cells to doxorubicin-induced growth Inhibition, G2-M arrest, and apoptosis. Clin Cancer Res 2002;8(11):3512–9. [PubMed: 12429642]

Ugurel S, Spassova I, Wohlfarth J, Drusio C, Cherouny A, Melior A, et al. MHC class-I downregulation in PD-1/PD-L1 inhibitor refractory Merkel cell carcinoma and its potential reversal by histone deacetylase inhibition: a case series. Cancer Immunol Immunother 2019;68(6):983–90. [PubMed: 30993371]

Ververis K, Hiong A, Karagiannis TC, Licciardi PV. Histone deacetylase inhibitors (HDACIs): multitargeted anticancer agents. Biologics 2013;7:47–60. [PubMed: 23459471]

von Tresckow B, Sayehli C, Aulitzky WE, Goebeler ME, Schwab M, Braz E, et al. Phase I study of domatinostat (4SC-202), a class I histone deacetylase inhibitor in patients with advanced hematological malignancies. Eur J Haematol 2019;102(2):163–73. [PubMed: 30347469]

Wang H, Zhang T, Sun W, Wang Z, Zuo D, Zhou Z, et al. Erianin induces G2/M-phase arrest, apoptosis, and autophagy via the ROS/JNK signaling pathway in human osteosarcoma cells in vitro and in vivo. Cell Death Dis 2016;7(6):e2247.

Wang X, Campoli M, Cho HS, Ogino T, Bandoh N, Shen J, et al. A method to generate antigen-specific mAb capable of staining formalin-fixed, paraffin-embedded tissue sections. J Immunol Methods 2005;299(1–2):139–51. [PubMed: 15896802]

West AC, Smyth MJ, Johnstone RW. The anticancer effects of HDAC inhibitors require the immune system. Oncoimmunology 2014;3(1).

Xiang J, Wan C, Guo R, Guo D. Is Hydrogen Peroxide a Suitable Apoptosis Inducer for All Cell Types? BioMed Res Int 2016;2016:7343965.

Zheng GXY, Terry JM, Belgrader P, Ryvkin P, Bent ZW, Wilson R, et al. Massively parallel digital transcriptional profiling of single cells. Nat Commun 2017;8:14049-.

Zheng H, Zhao W, Yan C, Watson CC, Massengill M, Xie M, et al. HDAC Inhibitors Enhance T-Cell Chemokine Expression and Augment Response to PD-1 Immunotherapy in Lung Adenocarcinoma. Clin Cancer Res 2016;22(16):4119–32. [PubMed: 26964571]

Zhou J, Wang G, Chen Y, Wang H, Hua Y, Cai Z. Immunogenic cell death in cancer therapy: Present and emerging inducers. J Cell Mol Med 2019;23(8):4854–65. [PubMed: 31210425]

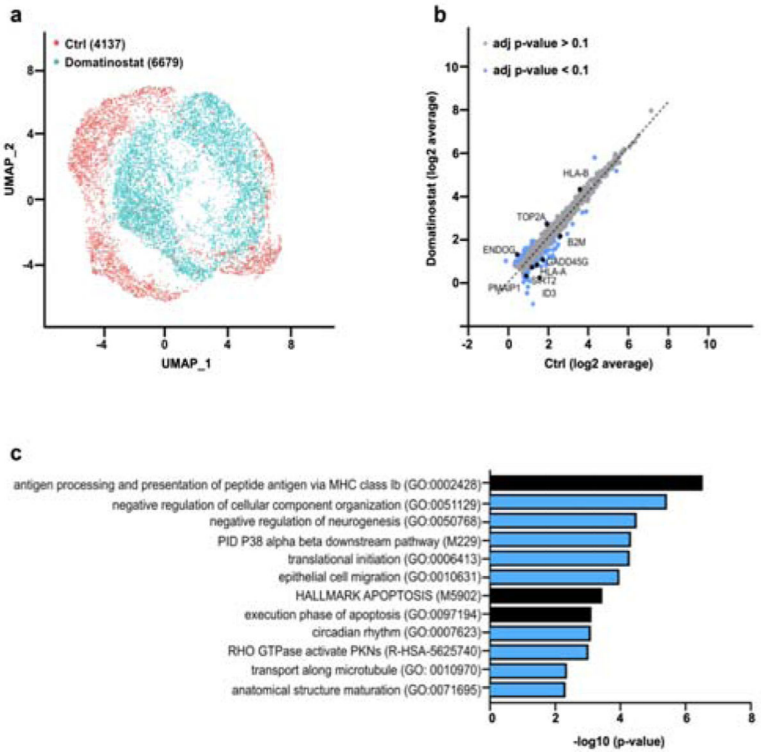


**Figure 1: Domatinostat induces global transcriptional changes in MCC cells.**

WaGa cells were either treated with domatinostat (2.5 μM, 24 hours) or solvent control before being subjected to single-cell RNA-seq. **(a)** Uniform Manifold Approximation and Projection (UMAP) of single-cell gene expression in WaGa cells annotated by treatment. **(b)** Comparison of average single-cell gene expression of domatinostat-treated and control cells. Significantly deregulated genes (adjusted *p*-value < 0.1) are labeled blue. (**c**) Metascape analysis of significantly enriched pathway terms in differentially expressed genes.

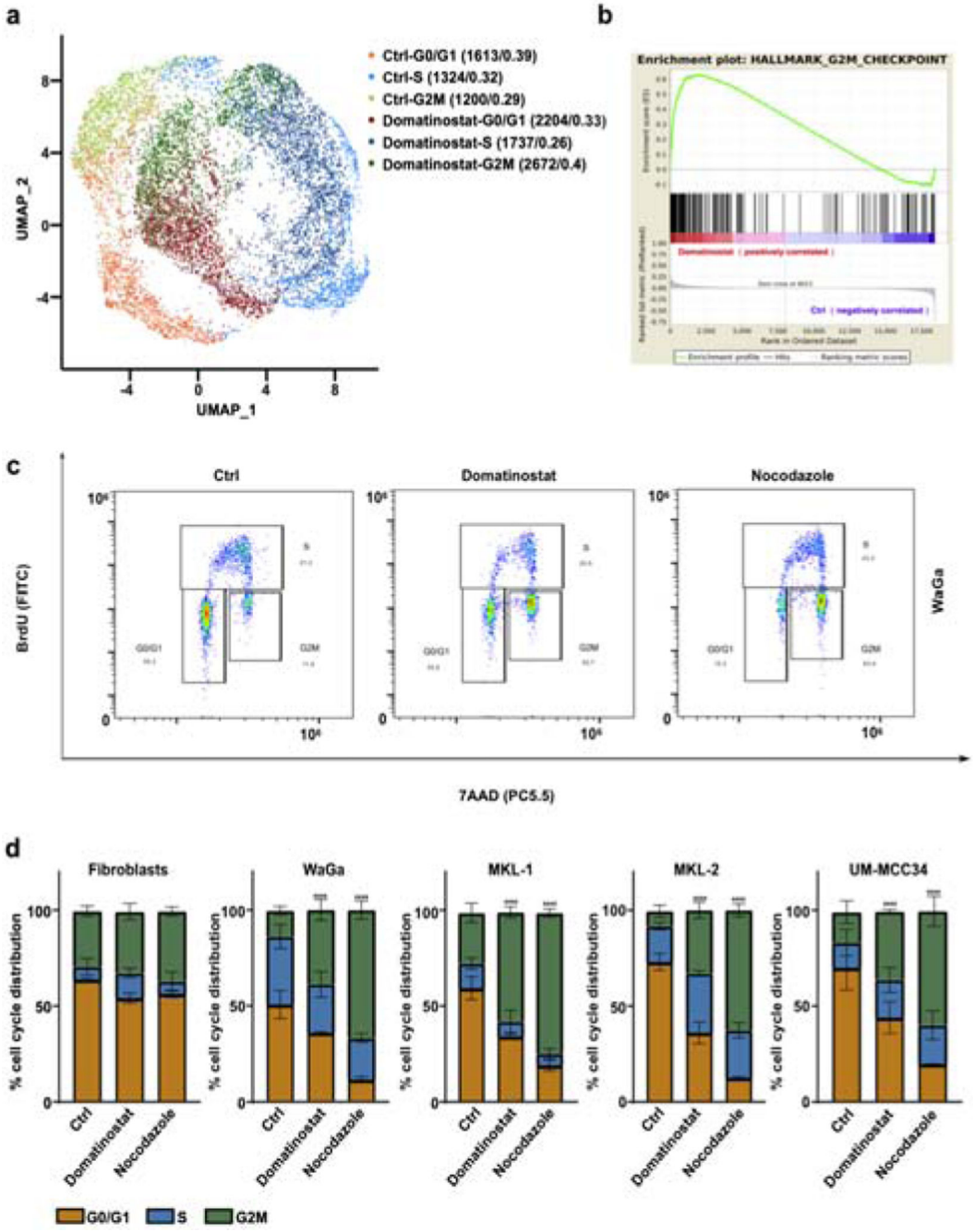


**Figure 2: Domatinostat promotes G2M cell cycle arrest.**

(**a**) UMAP visualization of single cell gene expression in WaGa cells after domatinostat treatment (2.5 μM, 24 hours) and solvent controls. Cells were annotated by cell cycle phase and treatment condition. Quantification of cells in the different cell cycle phases were given as absolute numbers and as fractions. (**b**) Pre-ranked Gene Set Enrichment analysis (GSEA) of the hallmark G2M checkpoint gene set for differentially expressed genes sorted by log2-fold change between domatinostat and solvent treated control cells (NES=1,91; FDR<0.001). **(c)** Cell cycle analysis by BrdU incorporation and 7-AAD staining of WaGa

cells treated 48 hrs. with domatinostat (2.5 μM) and solvent control or nocodazole (100 nM). **(d)** Quantification of cell cycle profiles in indicated cell lines, represented as mean + / −SD and presented as stacked bars (*P* values: ****, $P < 0.0001$). Experiments depicted in c and d were repeated twice.

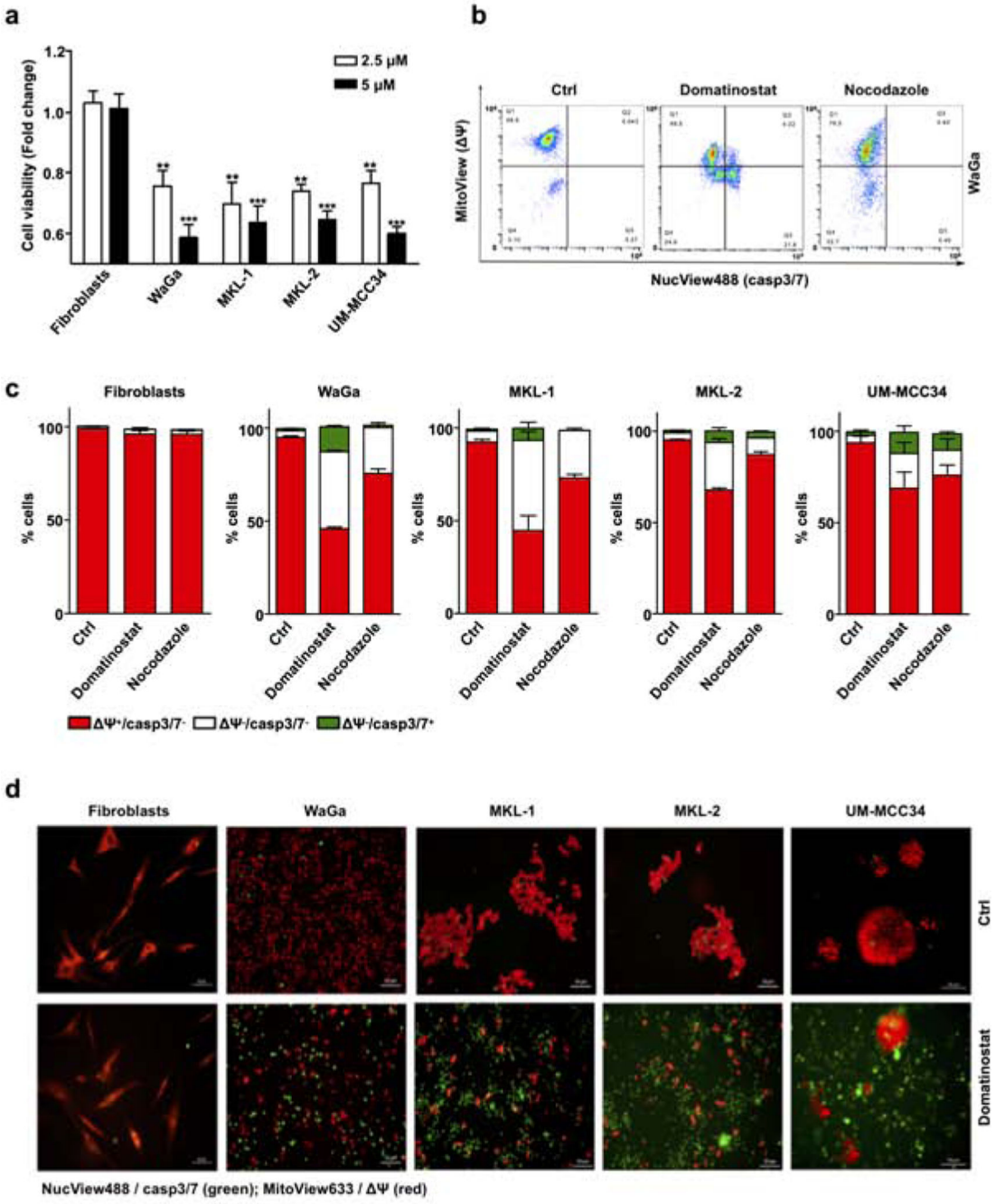


**Figure 3: Domatinostat treatment promotes apoptosis in MCC cells.**

**(a)** Viability of MCC cells and primary fibroblasts following a 24 hours treatment with indicated concentrations of domatinostat depicted as fold change as compared to solvent control. **(b-d)** In the NucView 488/MitoView 633 Apoptosis Assay, healthy cells with an intact mitochondrial membrane potential (ΔΨm) are stained with MitoView 633 (red), while late apoptotic cells (active caspase 3/7) are stained with NucView 488 (green). MCC cell lines and primary fibroblasts were treated with solvent control, 2.5 µM domatinostat or 100 nM nocodazole for 24 hours at 37°C. Visualization by flow cytometry **(b)** or fluorescence

microscopy **(d)**. Quantification of flow cytometry analysis is given in **(c)** as mean + / − SD and presented as stacked bars (whiskers: min to max) (P values: **, $P < 0.01$; ***, $P < 0.001$; ****, $P < 0.0001$). All experiments were repeated at least twice.

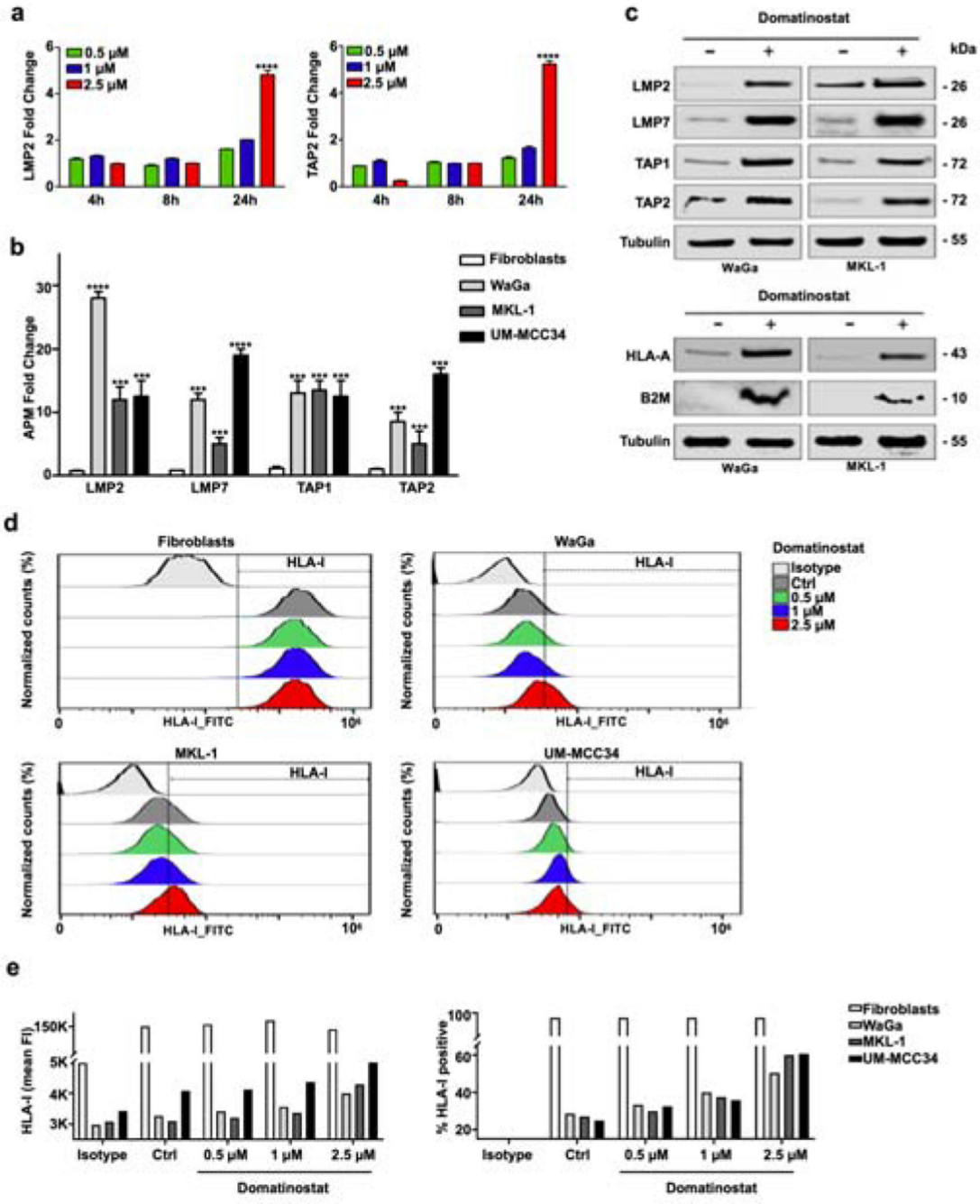


**Figure 4: Domatinostat induces expression of APM component gene expression and MHC class I surface expression by MCC cells.**

**(a)** WaGa cells were treated with the indicated concentrations of domatinostat for 4, 8 and 24 hours at 37 °C. Gene expression fold change to solvent controls of LMP2 and TAP2 detected by RT-PCR are depicted. **(b)** TAP1, TAP2, LMP2 and LMP7 mRNA expression in MCC cells and primary fibroblasts treated for 24 hours at 37 °C with 2.5 µM domatinostat was measured by RT-qPCR. Only living cells were included in the experiments. Gene expression fold change is depicted as mean + / − SD (**, $P < 0.01$; ***, $P < 0.001$; ****, $P <$

0.0001). **(c)** TAP1, TAP2, LMP2, LMP7, HLA-A and β2-microglobulin (B2M) protein expression in WaGa and MKL-1 cells treated with 2.5 μM domatinostat for 24 hours at 37 °C; β-tubulin was used as a loading control. Viable cells were enriched by Ficoll purification for preparation of whole cell lysates. **(d)** Dose dependent up-regulation of HLA class I (HLA-ABC) cell surface expression. Cells were treated with the indicated concentrations of domatinostat for 24 hours at 37 °C. **(e)** Quantification of HLA-I expression showing mean fluorescence intensity (FI, left) and % of HLA-I positive cells (right). All experiments were at least repeated twice.